NASA TECHNICAL NOTE

NASA TN D-8156

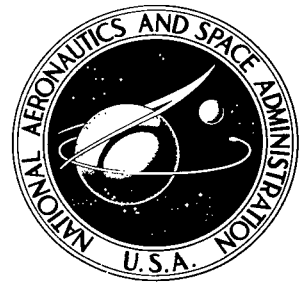

NASA TN D-8156

EXPLORATORY STUDY OF TRANSIENT UNSTART PHENOMENA IN A THREE-DIMENSIONAL FIXED-GEOMETRY SCRAMJET ENGINE

Allan R. Wieting

Langley Research Center
Hampton, Va. 23665

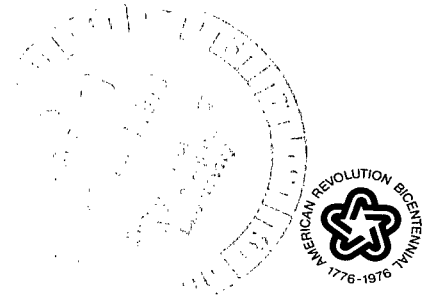

NATIONAL AERONAUTICS AND SPACE ADMINISTRATION • WASHINGTON, D. C. • MARCH 1976

1. Report No. NASA TN D-8156	2. Government Accession No.	3. Recipient's Catalog No.
4. Title and Subtitle EXPLORATORY STUDY OF TRANSIENT UNSTART PHENOMENA IN A THREE-DIMENSIONAL FIXED-GEOMETRY SCRAMJET ENGINE		5. Report Date March 1976 6. Performing Organization Code
7. Author(s) Allan R. Wieting		8. Performing Organization Report No. L-10643 10. Work Unit No. 505-02-12-01
9. Performing Organization Name and Address NASA Langley Research Center Hampton, Va. 23665		11. Contract or Grant No.
12. Sponsoring Agency Name and Address National Aeronautics and Space Administration Washington, D.C. 20546		13. Type of Report and Period Covered Technical Note 14. Sponsoring Agency Code
15. Supplementary Notes		

16. Abstract

The NASA Langley Research Center has initiated a research program which is focused on the structural and thermal design of a hydrogen-fueled regeneratively cooled three-dimensional fixed-geometry scramjet. A critical load that must be accommodated by the engine structure is the pressure load that occurs if the engine should thermally choke and unstart. An exploratory study was conducted at Mach 5.3 in the 7-inch Mach 7 pilot tunnel at the Langley Research Center to investigate the unstart phenomena and to provide the experimental data base required to predict the design pressure loads. The test results indicate that the peak pressures occurred during the transient unstart and not during steady-state started or unstarted flow conditions. The local peak pressures can be conservatively predicted by normal shock wave theory as the peak approaches the pressure that would exist behind a stationary normal shock with an upstream Mach number equal to the area weighted local Mach number for the normal started condition.

17. Key Words (Suggested by Author(s))
Air-breathing propulsion
Scramjet
Hypersonics

18. Distribution Statement
Unclassified – Unlimited

Subject Category 07

19. Security Classif. (of this report)	20. Security Classif. (of this page)	21. No. of Pages	22. Price*
Unclassified	Unclassified	18	$3.25

*For sale by the National Technical Information Service, Springfield, Virginia 22161

EXPLORATORY STUDY OF TRANSIENT UNSTART PHENOMENA IN A THREE-DIMENSIONAL FIXED-GEOMETRY SCRAMJET ENGINE

Allan R. Wieting
Langley Research Center

SUMMARY

The NASA Langley Research Center has initiated a research program which is focused on the structural and thermal design of a hydrogen-fueled regeneratively cooled three-dimensional fixed-geometry scramjet. A critical load that must be accommodated by the engine structure is the pressure load that occurs if the engine should thermally choke and unstart. Because of the complexity of engine geometry and flow, the unstarted flow condition could not be rigorously defined by analysis. Consequently, an exploratory study was conducted at Mach 5.3 in the 7-inch Mach 7 pilot tunnel at the Langley Research Center to investigate the unstart phenomena and to provide the experimental data base required to predict the design pressure loads. The test results indicate that the peak pressures occurred during the transient unstart and not during steady-state started or unstarted flow conditions. The local peak pressures were as high as 20 times the started local pressure levels. The transient pressure rise was reduced by approximately 40 percent when the geometric contraction ratio was increased from 2.6 to 4 by the addition of a diamond-shaped strut in the throat; however, the peak pressure levels remained essentially unchanged. The local peak pressures can be conservatively predicted by normal shock wave theory as the peak approaches the pressure that would exist behind a stationary normal shock with an upstream Mach number equal to the area weighted local Mach number for the normal started condition.

The peak pressure ratios experienced in scramjet ducts are a function of the free-stream Mach number, engine geometry, and compressive efficiency of the inlet system. Although the measured pressure ratios presented are correct only for the inlet geometry tested, they are indicative of the transient pressure levels that might be expected in any highly efficient inlet duct and the pressure levels must be accounted for in the structural design of inlet-duct systems.

INTRODUCTION

The NASA Langley Research Center has initiated a research program (ref. 1) which is focused on the development of airframe-integrated scramjet concepts. (See fig. 1.) As

part of this program, the thermal-structural design of a hydrogen-fueled regeneratively cooled three-dimensional fixed-geometry scramjet was undertaken to obtain realistic engine masses and cooling requirements (ref. 2).

A critical load that must be accommodated by the engine structure is the pressure load that occurs if the engine should thermally choke, thereby causing the engine to unstart. The dynamic characteristics of this or any other time dependent load may also be critical because the structural configuration consists of flat panels (walls) and slender winglike members (fuel-injection struts). These configurations have low flexural rigidity, relative to other structural configurations, and are thereby more easily excited (vibrated) by the airflow dynamics. The unstarted flow condition could not be rigorously defined by analysis because of the complexity of engine geometry and flow. Consequently, a test program was undertaken to provide the experimental data for analytical predictions of the design pressure loads. The tests, utilizing a simplified model of a single-engine module, were performed at a free-stream Mach number of 5.3 in the 7-inch Mach 7 pilot tunnel at the Langley Research (ref. 3). The unstart condition was simulated by insertion of a cylindrical pin downstream of the engine throat; the pin resulted in a flow area reduction of 60 percent. The results of this exploratory study are presented and compared with approximate analytical predictions.

SYMBOLS

The units used for the physical quantities defined in this paper are given both in the International System of Units (SI) and parenthetically in the U.S. Customary Units. Factors relating the two systems are given in reference 4. These quantities were measured in the U.S. Customary Units and then converted to SI.

A	airflow area, m^2 (in^2)
h	engine inlet height, mm (in.)
M	Mach number
p	local static pressure, Pa (psia)
t	time, s
x	longitudinal distance from sidewall leading edge (see fig. 4), mm (in.)

δ flow deflection angle, deg

θ shock wave angle, deg

Subscripts:

x local condition at x

∞ free-stream condition ahead of engine

APPARATUS AND TESTS

Model

A geometrically simplified model (figs. 2 and 3) was utilized to simulate a single-engine module of the type shown in figure 1. Since the flow instability of interest occurs upstream of the engine throat, the engine geometry downstream of the inlet throat was considered to be of secondary importance and was therefore simulated by a rectangular duct. The engine geometry was further simplified by making the internal top surface flat, since the sidewalls serve as the primary compression surfaces. The model (see fig. 3) had an inlet height of 38 mm (1.5 in.), an inlet width of 30 mm (1.2 in.), and an overall length of 179 mm (7 in.). The sidewall leading edges were swept at 48° to the flow and had a wedge angle of 5.6°. A single removable strut was used to simulate the reduction in flow area of the three fuel-injection struts of the actual engine. The strut was diamond shaped and had an included angle of 30.2° and a chordwise length of 23 mm (0.9 in.). The strut was located in the same position as the center strut in the actual engine and was swept at 48° to the free-stream flow. The geometric contraction ratio could be varied from 2.6 to 4 by installing the strut. Engine unstart was initiated by inserting a cylindrical pin 25 mm (1 in.) from the trailing edge of the top surface completely across the duct and orthogonal to the cowl surface. The pin resulted in a geometric flow area reduction of 60 percent. The pin insertion time was varied from 1.5 ms to 30 ms.

Instrumentation

Instrumentation consisted of strain-gage and inductance type pressure transducers located as shown in figure 4. Strain-gage type transducers were located in eight places on the starboard sidewall. Inductance type transducers were located on the port sidewall only. The strain-gage type transducers had a frequency response of approximately 100 Hz, and the inductance type transducers had a response which was flat to 400 Hz and 3 dB down at 1600 Hz.

Data were recorded on a high-speed digital system capable of recording 100 channels at a sampling rate of 200 frames (one frame being all 100 channels) per second. This setup was sufficient to record data with a frequency response up to 40 Hz. For higher frequency data, transducer outputs can be paralled to additional channels (maximum of 50) to obtain a sampling rate up to 10 000 frames per second, which is sufficient for recording data with a frequency response of 2000 Hz. Because of the limited data channels and the frequency-response requirements, the output of only two inductance gages could be recorded simultaneously.

Facility and Tests

The tests were conducted at a free-stream Mach number of 5.3 in the 7-inch Mach 7 pilot tunnel at the Langley Research Center. The facility, shown schematically in figure 5, is capable of simulating flight conditions for altitudes from 26 to 41 km (84 000 to 135 000 ft). Details on the facility and its operating range can be found in reference 3.

For these tests, the tunnel was operated at a total temperature of 290 K (530 R) and at free-stream dynamic pressures of 22.0 and 43.6 kPa (460 and 910 psf). Static and pitot pressure measurements indicated a nominal Mach number of 5.3 at the engine inlet for these test conditions.

Model configurations with and without the strut were tested at various pin insertion rates and both dynamic pressure levels. The test procedure was to establish the tunnel flow test conditions, insert the model, establish engine steady-state flow conditions with the inlet "started" (i.e., engine capturing the maximum airflow for the test condition and with supersonic flow in the inlet), insert the pin to "unstart" the engine, and then retract the model. This procedure was repeated for each test.

RESULTS AND DISCUSSION

Engine Model Without Strut

Unstart pressures.- Three distinctly different pressure-time profiles were obtained along the center line of the engine sidewalls, as indicated in figure 6. (Each profile includes three pressure levels: steady state started, "transient" unstart, and steady state unstarted. At $x/h = 1.3$ and 1.7, a simple monotonically increasing profile was obtained with the unstarted level approximately 4 times the started level. However, a radically different dome-shaped profile was also obtained at $x/h = 1.7$. This dome-shaped profile, which also occurred at $x/h = 2.0$, is characterized by a pressure that increased monotonically to a peak value of approximately 20 times the started level, then decayed monotonically to a level approximately 4 times the started level. At $x/h = 2.3$ (inlet area) and at $x/h = 3.0$ (constant area section), a plateau-shaped profile was

obtained. The peak pressure occurred during the transient unstart and was approximately 10 times the started level. The steady-state unstarted level was about 3 times the started level.

Three significant observations can be made from these profiles: (1) the maximum pressures occur during the transient unstart, (2) the maximum pressure rise (ratio of maximum pressure to started pressure) downstream of $x/h = 1.7$ is comparable to the pressure rise that would occur across a normal shock wave, and (3) the variation in the transient profile from location to location suggests a variation in the transient shock system as the engine unstarts.

In order to more clearly illustrate the preceding observations and subsequent conclusions, distributions of the three pressure levels (steady state started, steady state unstarted, and peak transient) are presented in figure 7. The steady-state started pressures, which are predicted well by inviscid flow theory except at $x/h = 2.3$, are in all cases the lowest pressures recorded. The steady-state unstarted pressures, which are 2.5 to 7 times the steady-state started pressures, are the maximum pressures obtained upstream of $x/h = 1.7$. However, downstream of $x/h = 1.7$ the peak pressures along the sidewall occur during the transient unstart and are as high as 20 times the started pressure levels. As shown in the figure, these peak pressures approach the pressure level that would exist behind a stationary normal shock in a supersonic stream with a Mach number equal to the local area weighted Mach number. It should be noted that the data are presented in figure 7 without distinction as to pin insertion time and dynamic pressures since no discernible effect of these parameters was observed.

Unstart shock system.- The unstarting flow phenomena for this three-dimensional scramjet is most complicated, but the outstanding physical features can be explained. Assuming that a normal shock originates at the pin, the shock would propagate upstream until sufficient air could be spilled external to the cowl. The resulting postulated shock pattern is shown in figure 8 and was determined (neglecting boundary-layer effects) by utilizing the techniques outlined in reference 5. The flow passage blockage by the pin (60 percent) and the attendant total pressure loss of the resulting normal shock reduce the captured mass flow by 67 percent. The captured mass flow passes through a normal shock extending over the upper third of the inlet. The remaining airflow passes through a hyperbolic-shaped shock wave which originates at the junction of the dividing streamline and the normal shock. The shock position is dictated by the requirement that the spilled mass flow must pass between the shock and the cowl. For this unstarted condition (fig. 8) the shock system would originate approximately 89 mm (3.5 in.) downstream of the top surface leading edge (approximately 1 inlet height forward of the cowl) and would pass approximately midway between the pressure measurement locations at $x/h = 1.7$ and 2.0. Obviously, the methods (ref. 5) utilized in predicting the shock pattern (fig. 8)

preclude accurate location of the pattern for this inlet geometry; however, the predicted location does agree well with the apparent location indicated by the pressure levels (fig. 7). The variation of the pressure profile at $x/h = 1.7$ (fig. 6) is indicative of the flow instability since the normal shock occasionally propagated at least that far upstream. This postulated shock pattern (fig. 8) accounts for the peak transient pressure levels over the aft portion of the inlet; however, it does not explain the increased pressures in the forward portion of the inlet. In addition, the postulated shock pattern does not agree with schlieren photographs.

Typical sequenced schlieren photographs of an inlet transient unstart are shown in figure 9. (It should be noted that the model was inverted during testing – to minimize flow blockage to the tunnel airflow by the model – and that the airflow is from left to right.) The first photograph ($t_0 = 0s$) shows the steady-state conditions for the inlet started. The next 10 photographs, which show the flow conditions during the transient unstarting of the inlet, indicate increased flow spillage from the inlet (note change in cloudlike pattern emanating from the inlet base). The last photograph ($t_{11} = 0.0055s$), which shows the steady-state unstarted flow conditions, indicates that the terminal shock system is oblique and not as postulated in figure 8.

The apparent anomaly between figures 8 and 9 is attributed to the fact that the effects of shock boundary-layer interaction are not included in the analysis (ref. 5) which was employed in obtaining the shock pattern shown in figure 8. During unstart the normal shock in the inviscid portion of the stream imposes a large adverse pressure gradient (fig. 6) on the boundary layer. The boundary-layer flow does not have sufficient momentum to negotiate this adverse pressure gradient; consequently, the boundary layer thickens and probably separates from all surfaces. These boundary-layer effects lead to oblique shock waves emanating at the point of separation and intersecting the normal shock. Because of continuity requirements, a reflected shock occurs at the juncture of the normal and oblique shocks and results in a lambda (λ) shock pattern at the wall. Inasmuch as the steady-state unstarted pressures upstream of $x/h = 1.7$ (fig. 7) are higher than the started pressure levels, the boundary-layer separation probably propagates almost to the leading edges, as indicated by the pressure rise at $x/h = 0.33$ (fig. 7). As the boundary-layer separation moves upstream, the compression leg of the lambda shock would also move forward and, eventually, the normal shock portion would disappear.

Again, a simplistic shock pattern is postulated to aid in explaining the outstanding physical features of the unstarting phenomena. Assuming that the Mach number upstream of the oblique shock is 5.3 and that the pressure rise across the shock is 10 (the steady-state unstarted level (fig. 7)), the shock wave angle and the flow deflection angle would then be 34° and 24°, respectively. The shock pattern shown in figure 10 is attained and is shown to be in good agreement with the last schlieren photograph shown in figure 9.

Consequently, the transient shock pattern is postulated to originate as a normal shock at the pin and to propagate upstream to form the pattern shown in figure 8. Then the separation phenomenon causes the shock pattern to become more oblique, as shown in figure 10.

Pressure-pulse propagation velocity.- Because the critical structural loading is transient, other factors, in addition to the amplitude of the pressure pulse, become important in determining the engine structural response. These other factors are the rise rate and decay rate of the pressure pulse as well as the duration and propagation velocity of the pulse across the structure. Of course, the effect of the propagation velocity on the structural response is dependent on the stiffness and mass distribution of the structure, as these determine the structural vibration frequencies.

An indication of the pressure-pulse propagation velocity can be ascertained from the simultaneous pressure measurements attained along a 48° sweep line (fig. 11) and along the longitudinal center line (fig. 12). The original intent of the measurements shown in figure 11 was to indicate shock orientation. The results indicate that the shock is not swept 48°, which is the basic orientation of constant flow conditions in the started operating mode. In the region downstream of $x/h = 2.0$, the pressure-pulse velocity is probably dictated by the rate at which the normal shock is expelled. Then, from figure 11, a velocity of 27 m/s (87 ft/sec) is attained if a normal shock is assumed to traverse the longitudinal distance between pressure orifices in the 0.36-ms interval between initial disturbances. In the region upstream of $x/h = 2.0$, the pressure-pulse velocity is probably dictated by the rate at which the boundary-layer separation propagates upstream. Then, from figure 12, a velocity of 10 m/s (32 ft/sec) is attained from the longitudinal distance between orifices and the 2.6-ms interval between initial disturbances. An overall average velocity (includes effects of both normal shock and separation) of 23 m/s (75 ft/sec) is obtained from the unstart time interval ($\Delta t = 5$ ms) indicated in figure 9 if it assumed that the pulse travels the longitudinal distance between the cowl leading edge and the top surface leading edge (114 mm (4.5 in.)). Obviously the data are somewhat inconclusive in indicating the propagation velocity; however, the velocities obtained are of the same order of magnitude, and the flow behavior in the forward portion of the inlet appears to be dictated by the separation phenomena.

Further testing is required to define the dynamic characteristics of the unstart phenomena. Definition of these characteristics is especially critical for the strut design of this scramjet concept as the struts are slender structural members with low torsional and bending stiffnesses.

Engine Model With Strut

Typical pressure-time profiles obtained along the longitudinal center line of the engine sidewalls are shown in figure 13. The results are similar to the results for the

model without a strut in that (1) the maximum pressures occur during the transient unstart and (2) the peak transient pressures approach the level that would exist behind a normal shock wave at the local area weighted Mach number. However, some dissimilar results are observed by comparison of the results shown in figure 13 with those in figure 6, as follows:

(1) The pressure level characteristic of the normal shock does not extend as far forward. (This is attributed to the downward turning of the flow toward the cowl by the strut, which probably results in easier flow spillage.)

(2) The transient unstart pressure rise (ratio of peak pressure to started pressure) is decreased in the vicinity of the strut.

(3) The steady-state unstarted pressure is less than the steady-state started level in the vicinity of the strut.

The presence of an internal strut in the inlet throat area increased the geometric contraction and started pressure levels in the throat area. Because of the attendant reduction in the throat Mach number, the transient unstart pressure rise in the throat area was less for the engine model with the strut. However, the maximum pressure levels remained essentially unchanged.

CONCLUDING REMARKS

An exploratory study has been conducted in the 7-inch Mach 7 pilot tunnel at the Langley Research Center to investigate the unstart phenomena of a three-dimensional scramjet with the unstart initiated by physically blocking 60 percent of the engine flow. These tests were to provide the experimental data base for prediction of the peak pressure loads for the three-dimensional scramjet module. The tests were conducted at a nominal Mach number of 5.3 and dynamic pressures of 22.0 and 43.6 kPa (460 and 910 psf).

The experimental results, although limited by model size, by data acquisition capabilities, and by being strictly applicable to the three-dimensional scramjet, are indicative of the transient pressure levels that might be expected in any highly efficient inlet duct and must be accounted for in their structural design.

The results indicate that a normal, or nearly normal, shock propagates upstream from its origin to approximately 1 inlet height forward of the cowl where sufficient air can be spilled external to the cowl. The peak pressures occurring in the region downstream of this normal shock are as high as 20 times the started pressure levels. The peak levels can be conservatively predicted by normal shock wave theory as the peak pressure levels approach the pressure that would exist behind a stationary normal shock with an upstream

Mach number equal to the area weighted Mach number for the normal started condition. The adverse pressure gradient imposed on the boundary layer by the normal shock system results in boundary-layer separation. The boundary-layer separation appears to extend to the top and sidewall leading edges and causes the normal shock to form an oblique shock leg which propagates forward with the separation. This results in an apparent oblique terminal shock system which originates near the leading edge of the top surface of the engine. The attendant pressure levels are approximately 2.5 to 7 times the started levels, which are significantly less than the levels behind the normal shock.

The unstart process is highly transient with a shock speed in the range of 10 to 27 m/s (32 to 87 ft/sec). Since the critical structural loading is transient, the dynamic characteristics must be determined and properly accounted for in the structural design of the engine.

The presence of an internal strut in the inlet throat area increased the geometric contraction and started pressure levels in the throat area. Because of the attendant reduction in the throat Mach number, the transient unstart pressure rise in the throat area was less for the engine model with the strut. However, the maximum pressure levels remained essentially unchanged.

Langley Research Center
National Aeronautics and Space Administration
Hampton, Va. 23665
February 23, 1976

REFERENCES

1. Becker, John V.; and Kirkham, Frank S.: Hypersonic Transports. Vehicle Technology for Civil Aviation – The Seventies and Beyond. NASA SP-292, 1971, pp. 429-445.

2. Wieting, Allan R.; and Guy, Robert W.: Preliminary Thermal-Structural Design and Analysis of an Airframe-Integrated Hydrogen-Cooled Scramjet. AIAA Paper No. 75-137, Jan. 1975.

3. Wieting, Allan R.: Experimental Investigation of Heat-Transfer Distributions in Deep Cavities in Hypersonic Separated Flow. NASA TN D-5908, 1970.

4. Metric Practice Guide. E380-72, American Soc. Testing & Mater., June 1972.

5. Moeckel, W. E.: Approximate Method for Predicting Form and Location of Detached Shock Waves Ahead of Plane or Axially Symmetric Bodies. NACA TN 1921, 1949.

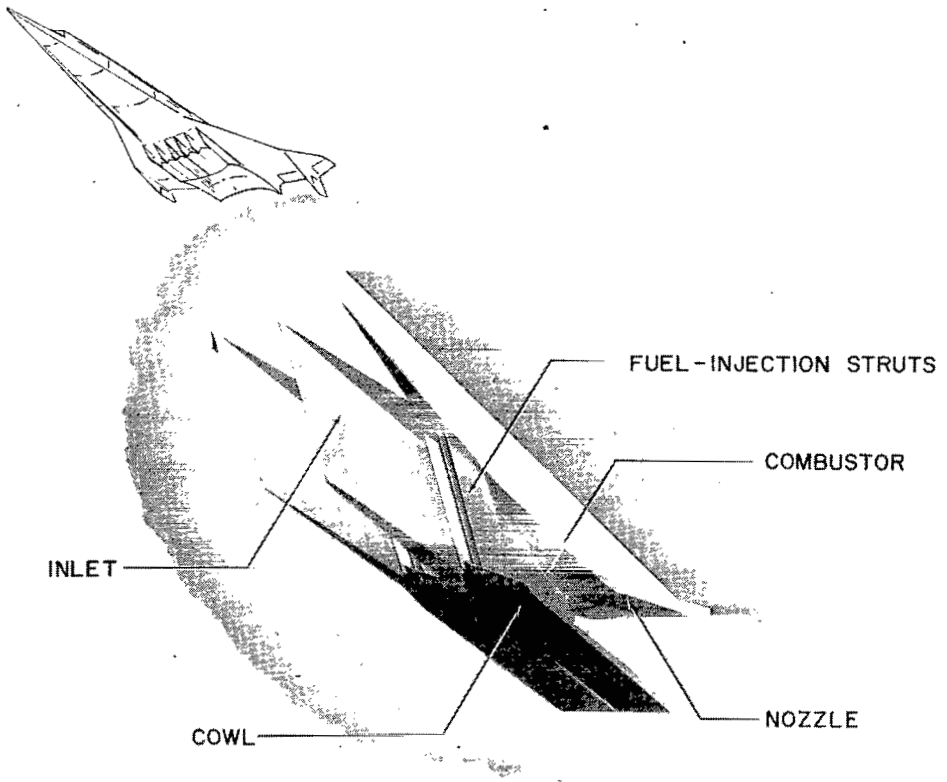

L-76-141

Figure 1.- Airframe-integrated scramjet.

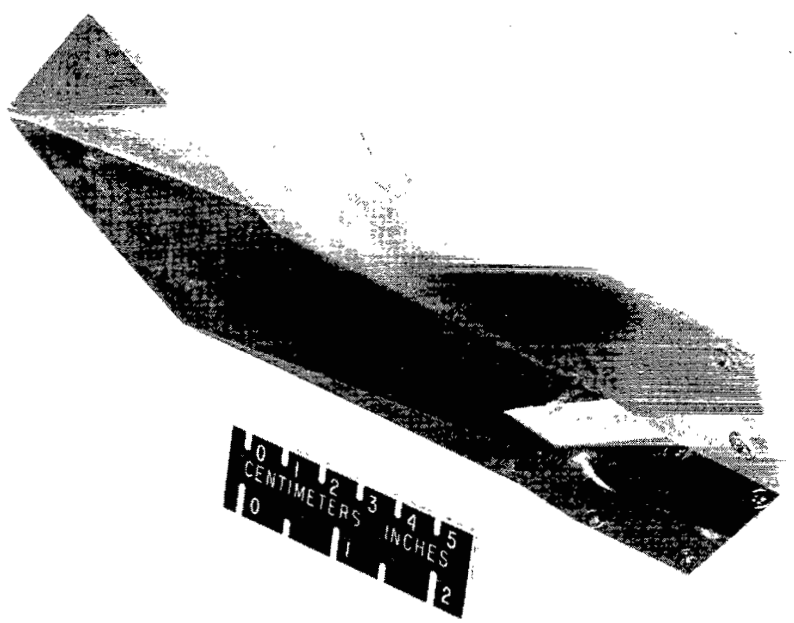

L-76-142

Figure 2.- Photograph showing oblique view of scramjet engine model.

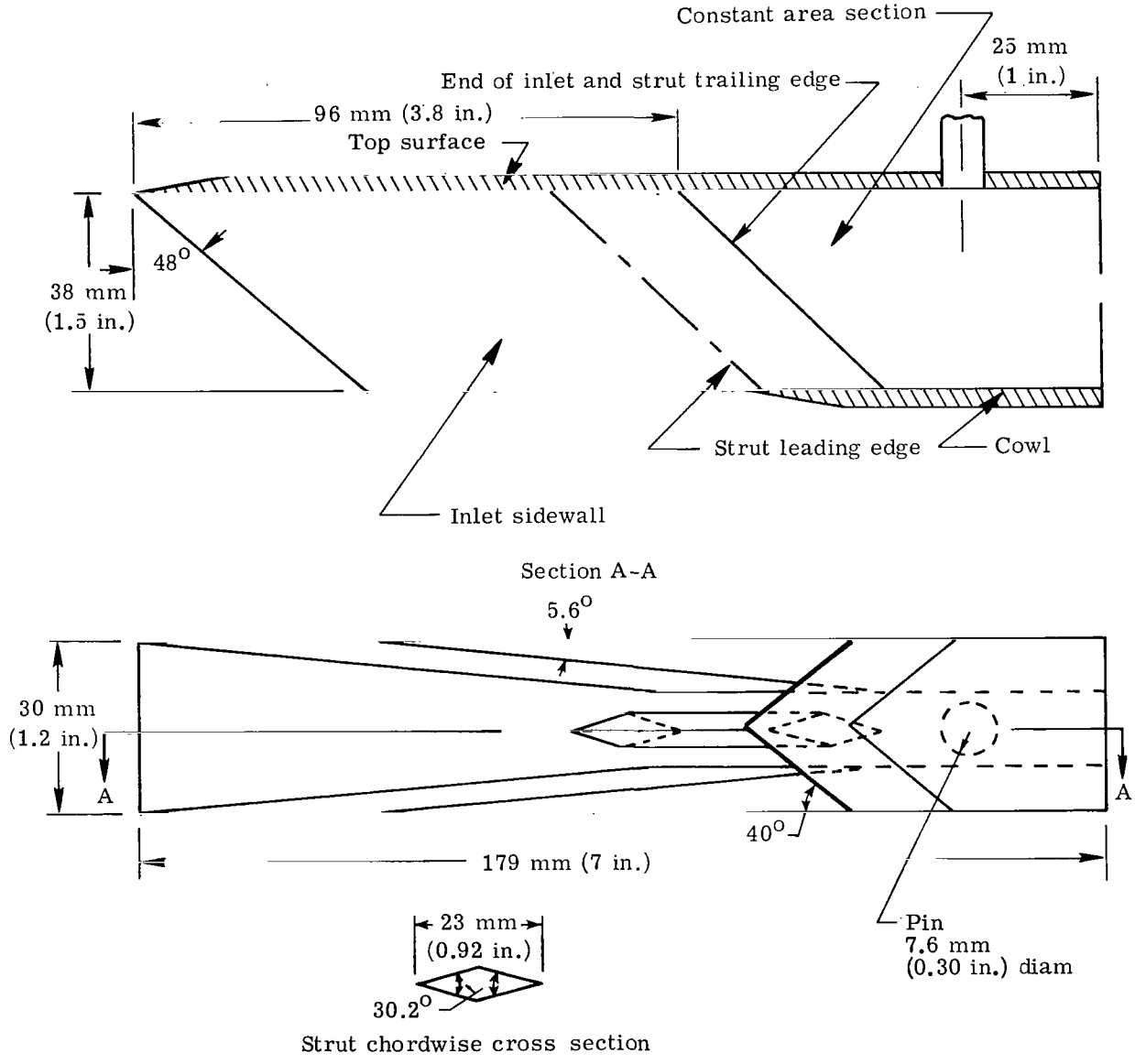

Figure 3.- Schematic of scramjet model.

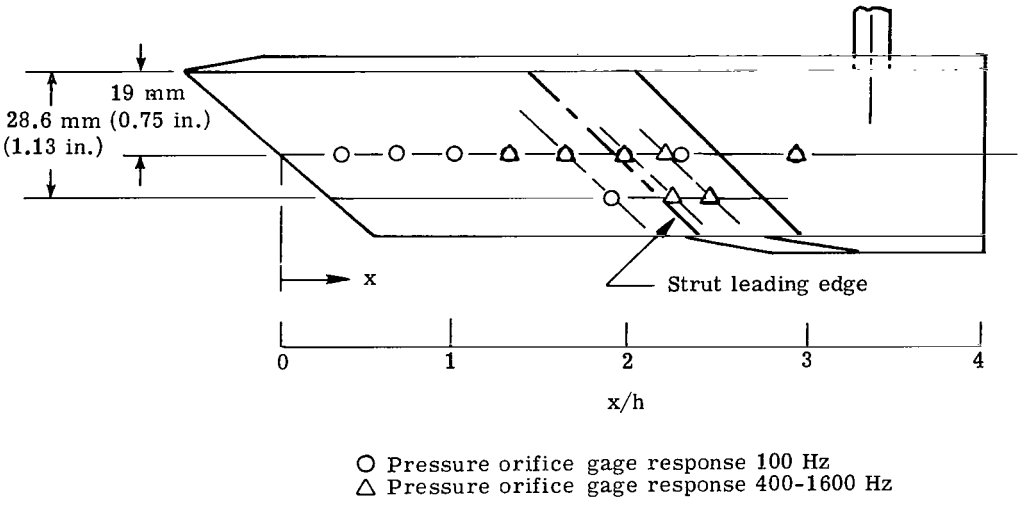

Figure 4.- Schematic showing instrumentation locations.

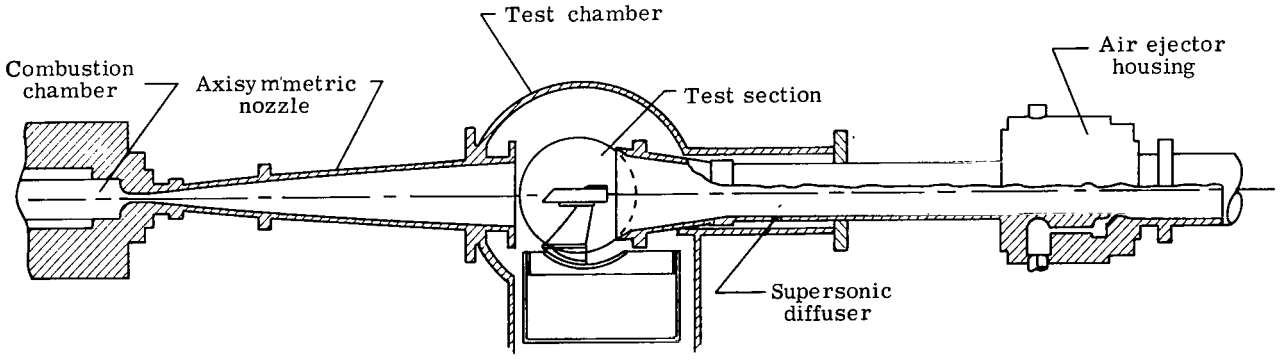

Figure 5.- Schematic of 7-inch Mach 7 pilot tunnel at the Langley Research Center.

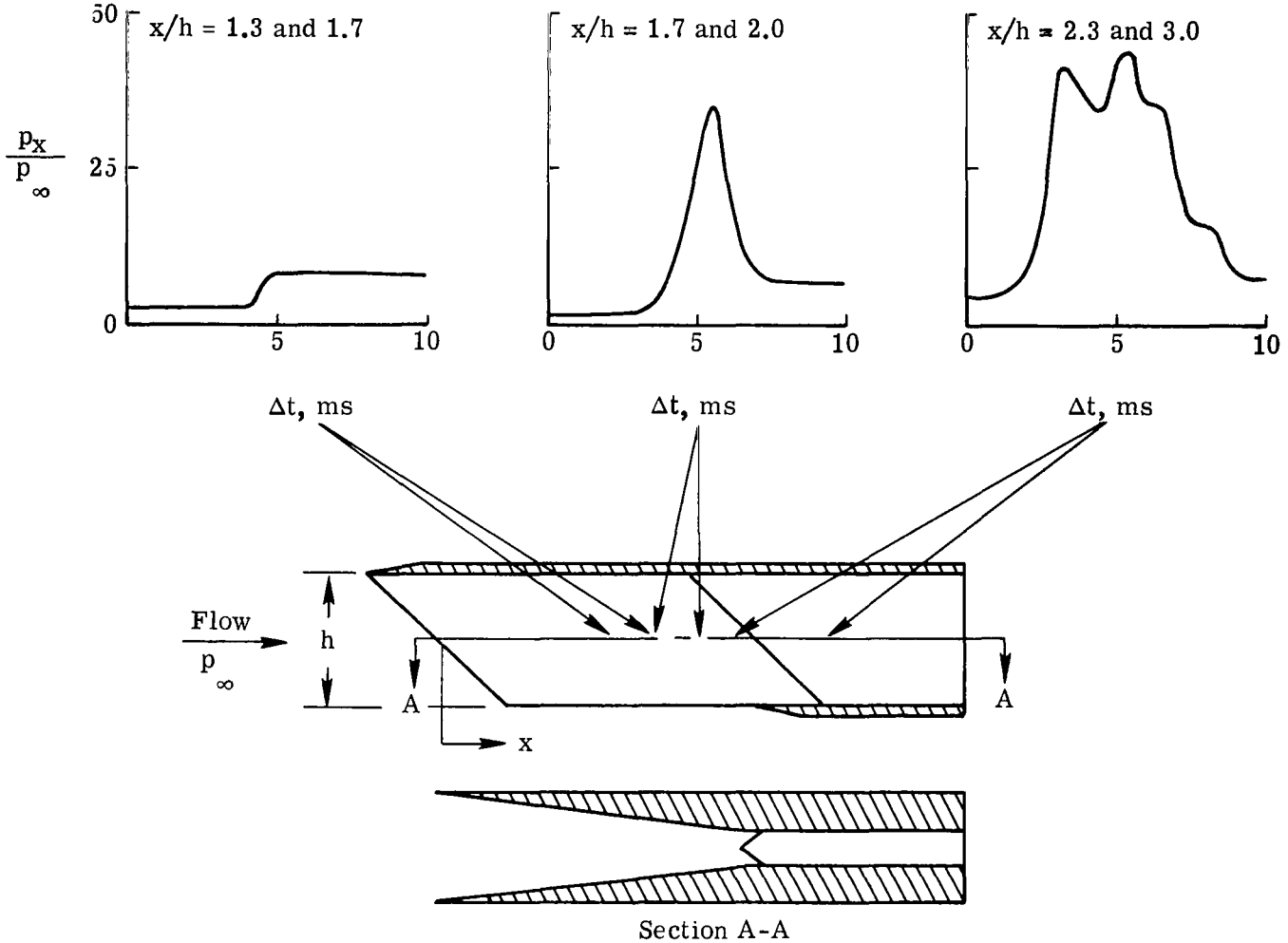

Figure 6.- Typical sidewall pressure-time profiles for model without strut.

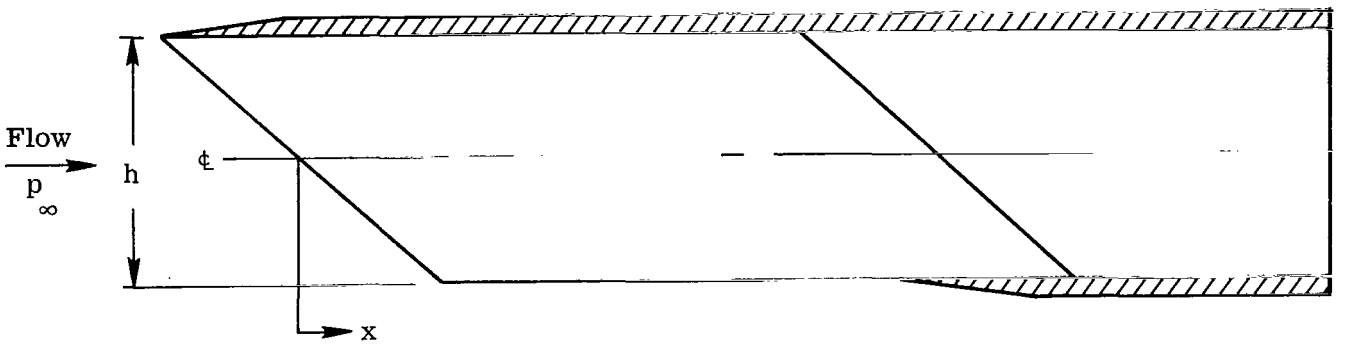

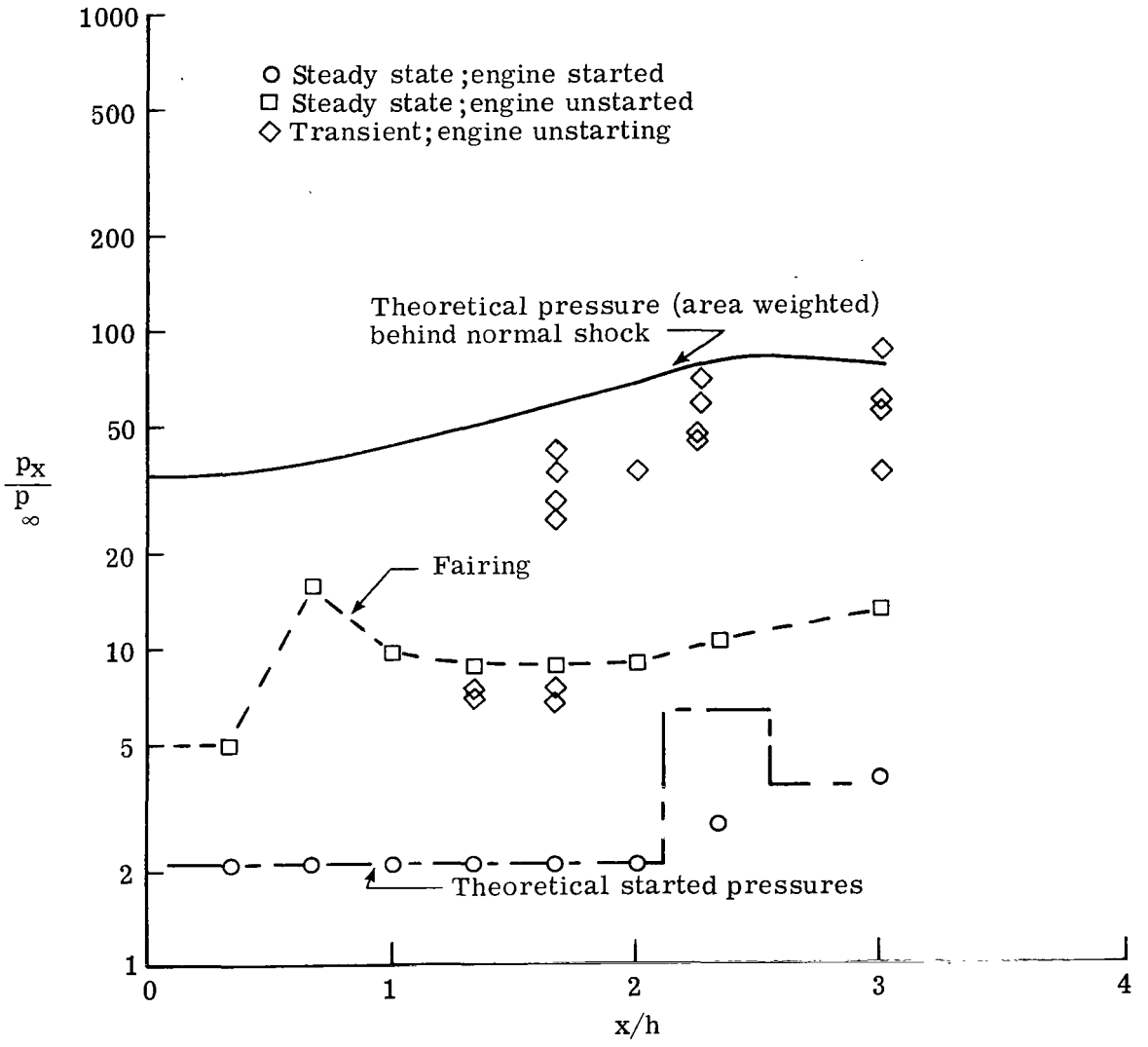

Figure 7.- Sidewall pressure distribution for model without strut.

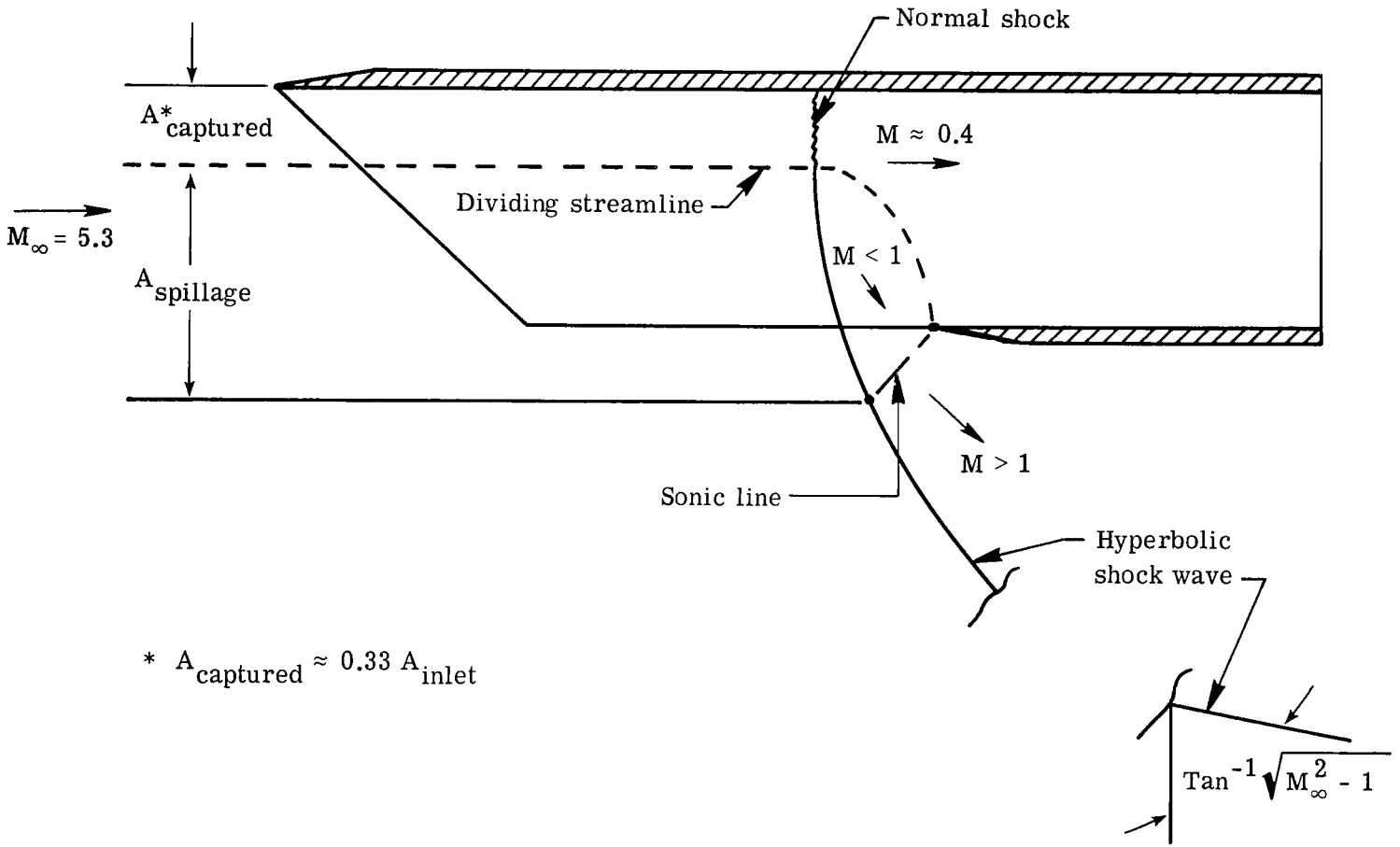

* $A_{captured} \approx 0.33\ A_{inlet}$

Figure 8.- Postulated transient unstart shock system, neglecting boundary-layer effects.

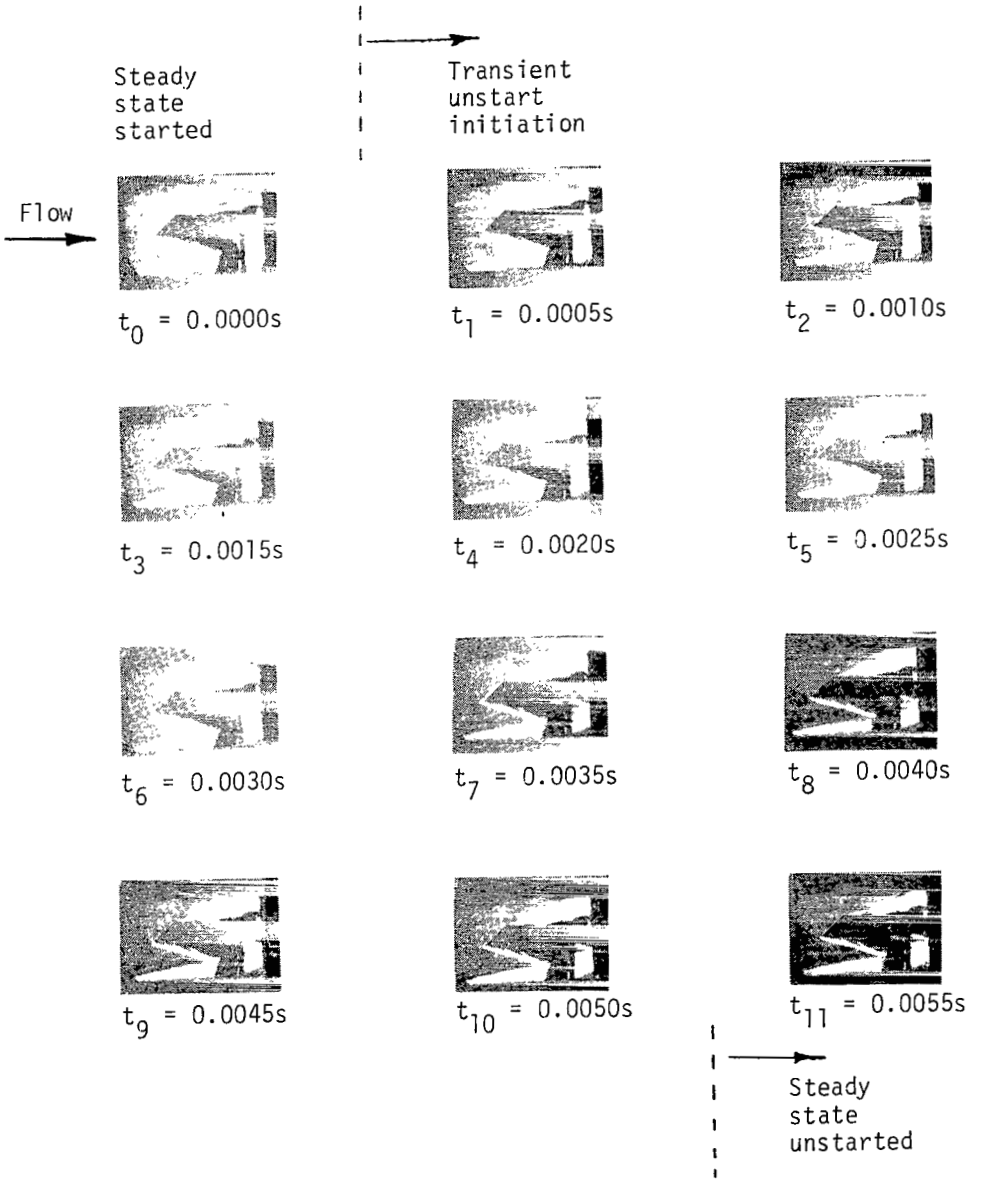

Figure 9.- Sequenced schlieren photographs of transient unstart.

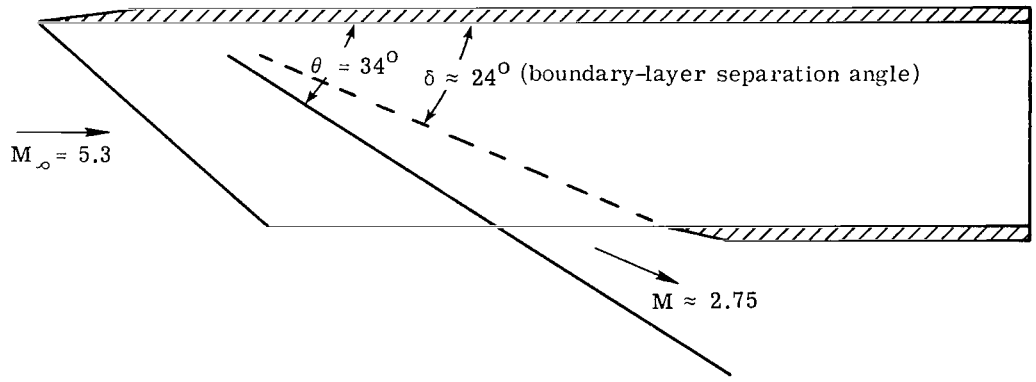

Figure 10.- Postulated terminal shock pattern for separated flow through engine.

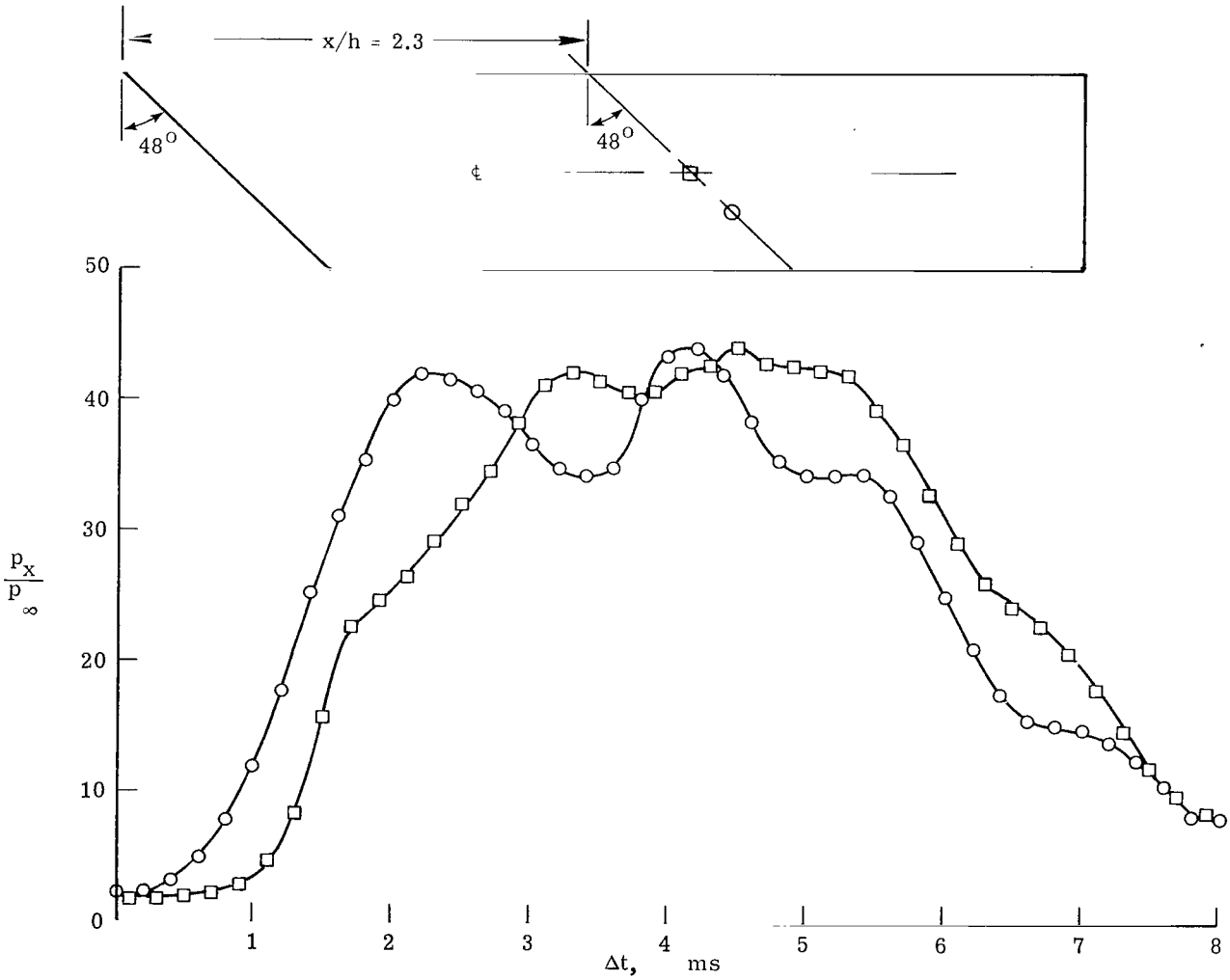

Figure 11.- Typical pressure histories obtained simultaneously on sweep line.

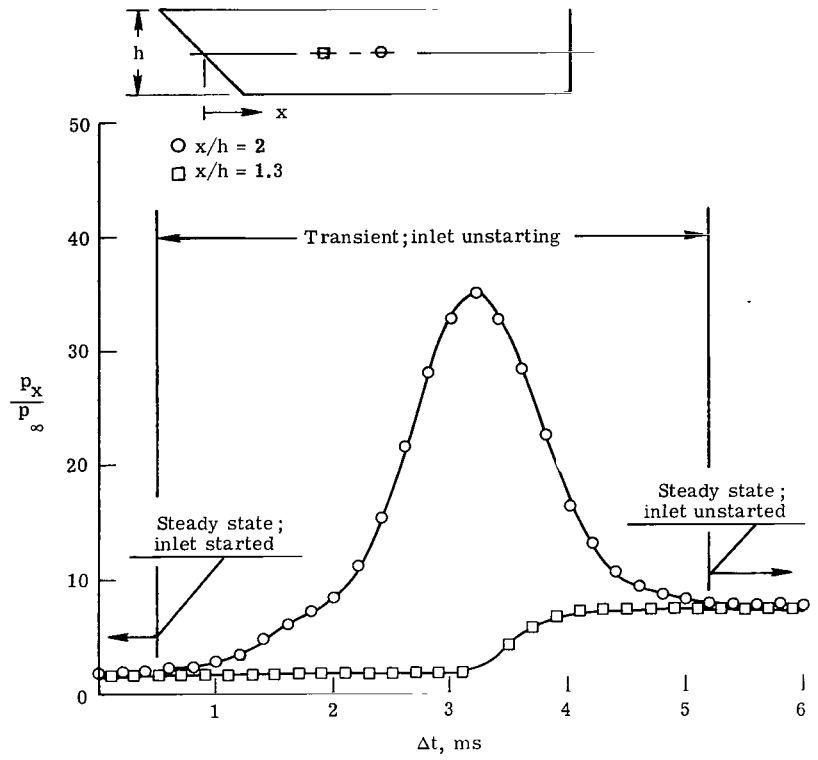

Figure 12.- Typical pressure histories obtained simultaneously on longitudinal center line.

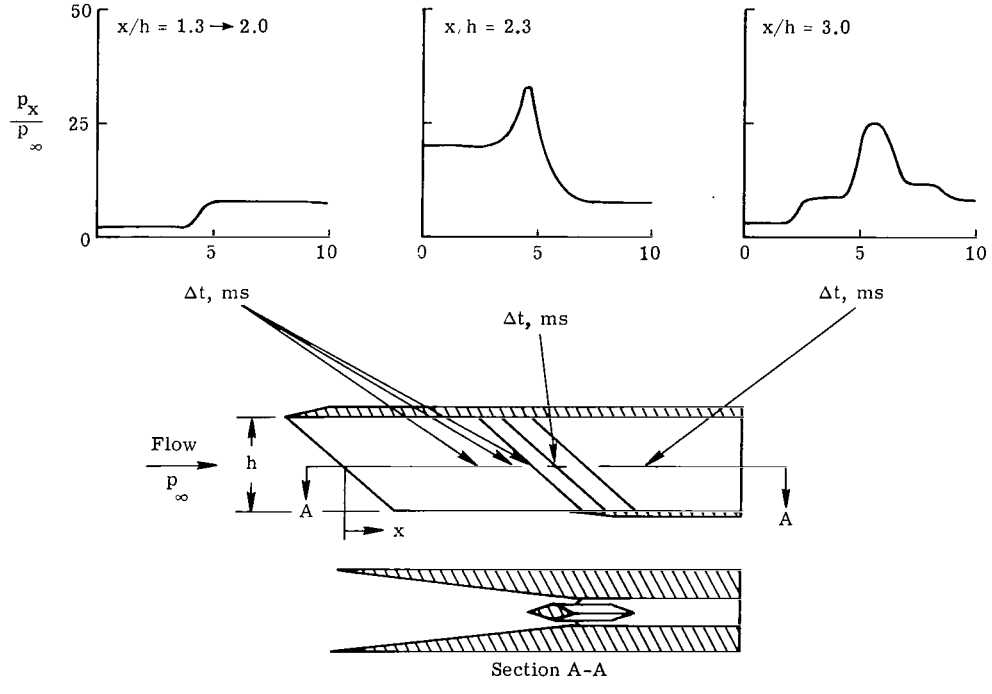

Figure 13.- Typical sidewall pressure-time profiles for model with strut.

"The aeronautical and space activities of the United States shall be conducted so as to contribute . . . to the expansion of human knowledge of phenomena in the atmosphere and space. The Administration shall provide for the widest practicable and appropriate dissemination of information concerning its activities and the results thereof."

—NATIONAL AERONAUTICS AND SPACE ACT OF 1958

NASA SCIENTIFIC AND TECHNICAL PUBLICATIONS

TECHNICAL REPORTS: Scientific and technical information considered important, complete, and a lasting contribution to existing knowledge.

TECHNICAL NOTES: Information less broad in scope but nevertheless of importance as a contribution to existing knowledge.

TECHNICAL MEMORANDUMS: Information receiving limited distribution because of preliminary data, security classification, or other reasons. Also includes conference proceedings with either limited or unlimited distribution.

CONTRACTOR REPORTS: Scientific and technical information generated under a NASA contract or grant and considered an important contribution to existing knowledge.

TECHNICAL TRANSLATIONS: Information published in a foreign language considered to merit NASA distribution in English.

SPECIAL PUBLICATIONS: Information derived from or of value to NASA activities. Publications include final reports of major projects, monographs, data compilations, handbooks, sourcebooks, and special bibliographies.

TECHNOLOGY UTILIZATION PUBLICATIONS: Information on technology used by NASA that may be of particular interest in commercial and other non-aerospace applications. Publications include Tech Briefs, Technology Utilization Reports and Technology Surveys.

Details on the availability of these publications may be obtained from:

SCIENTIFIC AND TECHNICAL INFORMATION OFFICE

NATIONAL AERONAUTICS AND SPACE ADMINISTRATION

Washington, D.C. 20546